Muscle-Ligament Interactions at the Human Knee (I)

— Maximum Isometric Leg Exercises —

Seonpil Kim*

(*Received February 2, 1998*)

The musculoskeletal model developed in this work is an improvement over previous models in two respects. First, the model is three-dimensional, and includes a detailed description of both patellofemoral and tibiofemoral mechanics. Second, and perhaps more significantly, the model takes into account the effects of both musculotendon properties and musculoskeletal geometry on calculations of ligament and articular-contact forces transmitted at the knee. The model presented here not only incorporates the force-length properties of all the major extensor and flexor muscles of the knee, but it also represents the path of each actuator more precisely. Simulations of maximum isometric knee extension and knee flexion were used to explain the variation in cruciate ligament loading at the knee resulting from the interaction between the external forces applied to the bones, the action of the muscles, and the articular-contact forces transmitted through the joint.

Key Words: Knee Model, Ligament Model, Musculoskeletal Model, Knee Extension, Knee Flexion

1. Introduction

A knowledge of the forces transmitted to the knee ligaments as a result of muscle activity is necessary for the design of ligament grafts and prosthetic replacements, and for the development of exercise regimens following ligament injury or repair.

A knowledge of the forces transmitted to the bones is also necessary for the design and surgical implantation of partial and total joint replacement. In view of the relatively high incidence of knee-ligament and joint replacement in the general population, studies of knee-ligament and joint function during activity are warranted.

A wealth of experimental data exist for the forces and strains produced in human knee ligaments *in vitro* (e. g., Markolf et al., 1990; Beynnon et al., 1995). These data are limited in one of two respects. First, ligament forces cannot be derived from data characterizing knee-ligament strain (Beynnon et al., 1995). Second, experiments carried out to define the forces borne by the knee ligaments have applied muscle forces whose magnitudes are well below the levels present during normal activity (Markolf et al., 1990). Numerous analytical studies also have been undertaken to study knee-ligament function under specific conditions of loading and constraint (see Hefzy and Grood, 1988 for details). Very few of these studies, however, have evaluated knee-ligament forces during activity (Collins and O'Connor, 1991; Zavatsky and O'Connor, 1993). Consequently, the pattern of cruciate- and collateral-ligament loading at the knee during activity has yet to be explained.

The specific goals of this paper are to (i) establish the magnitudes and patterns of forces induced in the cruciate and collateral ligaments of the knee during maximum isometric knee extension and knee flexion, (ii) determine the range of flexion over which the ACL and the PCL may be protected from strain during isolated contractions of the extensor and flexor muscles, and (iii)

* Technical Center Samsung Motors Inc. Yongin-City, Kyungki-Do, Korea

explain the overall patterns of cruciate and collateral ligament forces during maximum isometric knee extension and knee flexion.

2. Musculoskeletal model

In a previous study (Kim, 1998), a three-dimensional knee model was developed for the articular-surface geometry of the femur, tibia, and patella, for the cruciate and collateral ligaments of the knee. By incorporating the knee model into a four-segment thirteen muscle model of the human body, we simulated a series of maximum isometric knee extension and knee flexion exercises to determine the muscle, ligament, and articular contact forces transmitted at the knee as humans exert maximum voluntary effort during knee extension and knee flexion.

2.1 Tibiofemoral joint model

The geometry of the distal femur, proximal tibia, and patella was obtained from cadaveric data reported for an average-size knee. The patellar surfaces of the model femur and the posterior portion of the model femoral condyles were represented by fourth-order and second-order polynomials, respectively (see Kim, 1998 for details). The model tibial plateaux and model patellar facets were each approximated as sloped flat surfaces. The lateral tibial plateau was sloped 7° posteriorly and 2° laterally, while the medial tibial plateau was sloped 2° posteriorly and medially. The surfaces of the patellar facets were divided by a vertical ridge and inclined at an angle of 130° to one another.

Twelve elastic elements were used to describe the function of the ligamentous and capsular structures of the knee. The anterior cruciate ligament and posterior cruciate ligament were each represented by two bundles. The structures on the medial side of the knee were represented by five bundles. The lateral collateral ligament was modeled as one whole tissue. Two separate bundles were used to model the action of the posterior capsule of the knee. The origin and insertion sites of each model ligament were obtained from cadaveric data reported for an average-size knee.

Each ligament bundle was assumed to be elastic, and its mechanical behavior was represented by a nonlinear stress-strain curve. Specifically, the force in each model ligament bundle was assumed to be quadratic for low strains, and linear for strains beyond a prespecified point corresponding to twice the linear strain limit.

Unfortunately, no experimental data are available for the reference strains of knee ligaments. These parameters, together with the values of ligament stiffness, were determined by matching the overall stiffness and laxity of the model knee with experimental data reported in the literature.

2.2 Deformable contact

It is assumed that due to the presence of synovial fluid, the femoral condyles roll and slide on the tibial plateaux without friction. Deformation of the bones is calculated by modeling the behavior of cartilage as a thin elastic layer mounted on a rigid foundation that represents the underlying subchondral bone. The deformable-contact model calculates the contact force by integrating the assumed contact-pressure distribution over the deformed surface area. The resulting forces at the medial and lateral compartments of the knee are then included in the equations of motion in the same way as the concomitant ligamentous and muscle forces. No additional kinematical constraints are necessary when modeling deformable contact in this way. As a consequence, relative movements of the tibia and femur in the model are characterized by *six* degrees of freedom.

At the contact point, a common tangent plane can be found. This common tangent plane ensures that proper contact occurs between the surfaces at the point of contact (Fig. 1). To find the location of the contact point, two conditions, referred to as the *contact conditions,* must be satisfied. First, the tangents and normals to each surface at the contact point must be *parallel:*

$$\boldsymbol{t}_a \bullet \boldsymbol{n}_b = 0 \tag{1}$$

where $\boldsymbol{t}_a$ is the tangent vector to body A (femur) at the contact point, and $\boldsymbol{n}_b$ is the normal vector to body B (tibia) at the contact point. Second, the

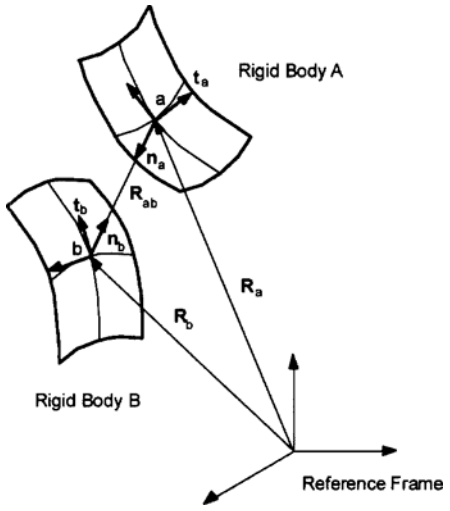

Fig. 1 The contact conditions for the deformable contact model at the tibiofemoral joint. Points a and b represent the points of first contact on bodies A and B, respectively. The vector from point a to point b must be directed along the common normal to both bodies.

tangents and normals to each surface at the contact point must be *collinear:*

$$t_a \bullet R_{ab} = 0 \tag{2}$$

where R_{ab} is the vector directed from the contact point on body A (femur) to the contact point on body B (tibia). The location of the contact point was found by solving Eqs. (1) and (2) simultaneously using a root-finding algorithm for nonlinear equations.

The geometry of the femur and tibia in the region of the point of first contact is approximated; the shape of each surface in the vicinity of the contact region is described by a second-order surface polynomial. When each of these surfaces is projected onto the tangent plane at the point of contact, the projected shape is an ellipse. Since the shape of the contact area is elliptical, the shape of the deformed volume is that of an *elliptic paraboloid.* The applied pressure distribution in the model is assumed to be paraboloidal. This pressure distribution is then integrated to give a closed-form, analytical solution for the resultant force transmitted at the medial and lateral sides of the tibiofemoral joint.

2.3 Knee-extensor mechanism

We assumed that the patella could be approximated as a massless body. This assumption is reasonable since the mass of the patella is negligible in comparison with the mass of either the thigh or the shank. The surfaces of the patellar facet and femoral groove were also assumed to be frictionless. Under these assumptions, only four forces act to equilibrate the patella at any given angle of the knee: the force applied by the quadriceps tendon, the force developed in the patellar ligament, and the two contact forces acting at the medial and lateral sides of the patellofemoral joint (Kim, 1998). Note that the force applied to the model patella by the quadriceps tendon is the resultant force developed by the four separate heads of the quadriceps muscles included in the model: rectus femoris (RF), vastus medialis (VMED), vastus intermedius (VINT), and vastus lateralis (VLAT).

To calculate the contact forces between the femur and patella, we neglected the effects of cartilage; the medial and lateral facets of the patella and the medial and lateral portions of the femoral groove were all modeled as rigid surfaces. Our model for patellofemoral contact, therefore, is different from that used to describe contact between the femoral condyles and the tibial plateaux. Equations (1) and (2) are used to calculate the location of the contact point at each side of the patellofemoral joint. The rigid-body contact condition ensures that no interpenetration takes place between the surfaces of the femur and patella at each contact point. Thus,

$$R_{ab} \bullet n|_{i=1,2} = 0 \tag{3}$$

where n is the common normal at the contact point for body A (patella) and body B (femur).

2.4 Model for musculotendon force

Each musculotendinous unit was modeled as a three-element, lumped-parameter, muscle, in series with tendon. The mechanical behavior of muscle was described by a Hill-type contractile element that models its force-length-velocity

property, a series-elastic element that models its short-range stiffness, and a parallel-elastic element that models its passive stiffness. Tendon was assumed to be elastic, and its mechanical behavior was modeled by a linear stress-strain (σ-ε) curve. Other assumptions implicit to the musculotendon models are that all sarcomeres in a given fiber are homogeneous, all muscle fibers reside in parallel and insert at the same pennation angle on tendon, and muscle volume and cross-section remain constant. For isometric contractions, a nonlinear, algebraic equation relates muscle activation (a), musculotendon length (L^{MT}), and musculotendon force (F^{MT}) (Pandy et al., 1990):

$$f_i(F_i^{MT}, L^{MT}, a_i) = 0 \quad (4)$$

For known values of muscle activation and musculotendon length, equation (4) may be used to compute the corresponding force in the musculotendon actuator. The length (LMT) of each musculotendon actuator in the model can be found once the relative displacements of the bones are known. The relative displacements of the bones are determined by the applied muscle forces in the model.

2.5 Musculotendon properties and musculoskeletal geometry

The model knee was actuated by thirteen musculotendinous units: four separate heads of the quadriceps muscles, four heads of the hamstrings, the medial and lateral heads of gastrocnemius (GASLAT and GASMED), gracilis (GRA), sartorius (SAR), and tensor fascia latae (TFL) (Fig. 2). The four heads of the quadriceps muscles included in the model were rectus femoris (RF), vastus medialis (VMED), vastus lateralis (VLAT), and vastus intermedius (VINT). The four heads of the model hamstrings were short head of the biceps femoris (BFSH), long head of biceps femoris (BFLH), semitendinosus (TEN), and semimembranosus (MEM).

The musculoskeletal geometry of the model (musculotendon origin and insertion sites) was defined on the basis of data reported by Friederich and Brand (1990) and Delp (1990). Parameters defining nominal muscle properties (i. e., maximum isometric force, pennation angle, and optimum muscle-fiber length) for each musculotendinous unit in the model were adapted from Delp (1990). We adjusted the maximum isometric force developed by each muscle and the resting lengths of the actuator tendons in the model until the maximum, isometric, torque-angle curves for flexion and extension of the model knee matched those obtained from human subjects performing maximum, voluntary, isometric contractions at the ankle, knee, and hip (see Kim, 1996 for details).

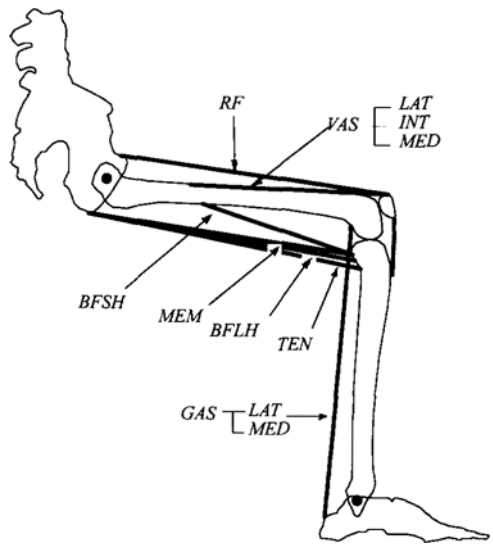

Fig. 2 Schematic of the musculoskeletal model used to simulate knee extension and knee flexion. The human body is modeled as a two-segment, spatial linkage, actuated by thirteen musculotendinous units. Tensor fasciae latae (TFL), gracilis (GRA), and sartorius (SAR) are included in the model but not shown for clarity.

3. Maximum Isometric Knee Extension and Knee Flexion Exercises

The lower extremity model was used to simulate a series of maximum isometric knee extension and knee flexion exercises. In this task, only relative movements of the femur, tibia, and patella are considered. Specifically, we assume that the

femur remains stationary relative to an inertial reference frame fixed on the ground. Biarticular muscles, such as rectus femoris and biceps femoris long head, which span both the knee and the hip, are attached to a stationary pelvis in the model. The hip angle in the model was specified according to the task being simulated. For maximum isometric knee flexion and knee extension in the model, as in the experiments, the hip angle was set to 60° of flexion. The ankle was held in the neutral (standing) position.

For a given value of knee flexion, maximum isometric knee extension (flexion) was simulated by fully activating all the extensor (flexor) muscles in the model, and simultaneously deactivating all the antagonists (i. e. co-contraction of the antagonist muscles was neglected in the model). Thus, only the passive forces developed by the antagonist muscles were taken into account in these calculations. The governing equations for the overall musculoskeletal model are:

$$G(\boldsymbol{q}_{tf}) + M_{lig}(\boldsymbol{q}_{tf}) F_{lig} + M_{tf}(\boldsymbol{q}_{tf}) F_{tf} + M_{pl}(\boldsymbol{q}_{tf}) F_{pl} + M_m(\boldsymbol{q}_{tf}) F^{MT} + \boldsymbol{E} = 0 \qquad (6)$$

where $M_{lig}(\boldsymbol{q}_{tf})$ is a 6×12 matrix which contains the moment arms of the model ligament bundles, each calculated about the origin of the tibial reference frame; $M_{tf}(\boldsymbol{q}_{tf})$ is a 6×2 matrix containing the moment arms of the contact forces acting at the medial and lateral sides of the tibiofemoral joint, each calculated about the origin of the tibial reference frame; $M_{pl}(\boldsymbol{q}_{tf})$ is a 6×1 matrix containing the moment arm of the patellar ligament force calculated about the origin of the tibial reference frame; $M_m(\boldsymbol{q}_{tf})$ is a 6×13 matrix which specifies the moments arms of all the muscles in the model, calculated about the origin of the tibial reference frame; Ftf are the tibiofemoral forces which act normal to the contacting surfaces on the medial and lateral sides of the joint; F_{lig} are the ligament forces acting on the tibia; $G(\boldsymbol{q}_{tf})$ is a 6×1 vector containing only gravitational terms; $\boldsymbol{E}$ is a 6×1 vector containing the restraining force applied to the tibia.

4. Human Experiments

Measurements of maximum isometric knee -extensor and knee-flexor muscle strength were used to scale the strength of the model to that of human subjects. Five healthy, young, adult males (age 26 ± 3 yr., height 177 ± 3 cm; weight 68 ± 6 kg) were chosen for a series of isometric knee extension and knee flexion exercises. All subjects were all free from any muscle or joint abnormality. Details of these experiments are reported by Shelburne and Pandy (1997). A brief description of the methodology is provided below.

A Biodex dynamometer was used to measure the net extensor and flexor torque at the knee for each prescribed angle of knee flexion. For all measurements, the subject was seated with the hips flexed to 120°, and with the right leg strapped firmly to the arm of Biodex dynamometer. Straps were tightened across the thigh near the hip and the knee to ensure that the thigh segment remained horizontal throughout testing. Prior to data collection, the subject familiarized himself with the testing protocol by performing a series of isometric contractions of the knee extensor and knee flexor muscles. The subject was then instructed to exert maximum, voluntary effort in knee extension and knee flexion separately. During each set of experiments, knee torque was recorded from 90° of flexion to full extension in increments of 10°, with two contractions given at each knee angle. Each contraction lasted three seconds.

5. Maximum Isometric Knee Extension

5.1 Extensor torque

The maximum torques calculated for isometric extension of the model knee fell within the range of the values measured for the subjects (Fig. 3, compare heavy solid line with shaded region). The model and the subjects generated peak extensor torque at around 65° of knee flexion. Peak knee extension torque in the model is determined primarily by the ratio of the tendon rest length to optimum muscle-fiber length for each of the

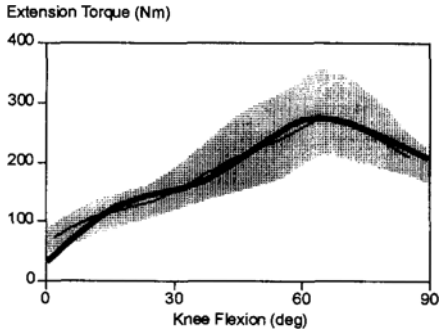

Fig. 3 Maximum, isometric, knee-extensor, torque-angle curves for the model (heavy solid line) and for human subjects (shaded region). The thin solid line represents the mean of all the experimental measurements. The shaded region represents ± 1 standard deviation of the total extensor torques measured for the subjects during maximum, voluntary, isometric contractions for the quadriceps.

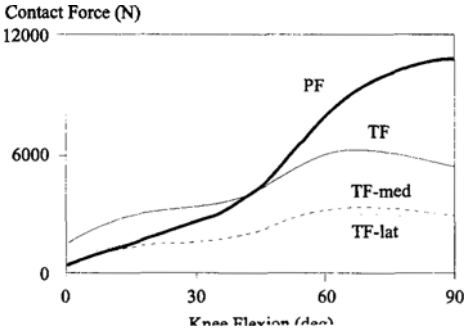

Fig. 4 Quadriceps muscle force calculated for maximum isometric extension of the model knee. Quad (heavy solid line), represents the resultant of the forces developed by the four heads of the quadriceps muscles included in the model.

quadriceps muscles (VLAT, VINT, VMED, and RF). For the values assumed in the model, the forces developed by the uniarticular VLAT, VINT, and VMED muscles dominate the shape of the torque-angle curve (Fig. 4, compare VLAT, VMED, and VINT with Quad). At small angles of flexion, total quadriceps force is dominated by the force developed in VMED (compare VMED with VINT and VLAT from full extension to 30 ° of flexion). As knee flexion increases, however, the forces developed by VLAT and VINT represent a greater proportion of the total force

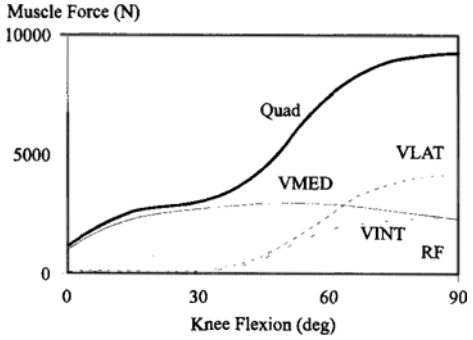

Fig. 5 Articular contact forces for maximum isometric extension of the model knee. Resultant force acting at the patellofemoral joint in the model (PF, heavy solid line). Resultant force acting at the tibiofemoral joint in the model (TF, light solid line). The forces acting at the medial and lateral sides of the tibiofemoral joint are also shown.

transmitted to the quadriceps tendon (compare VINT, VLAT, and VMED with Quad for the range 60-90° of flexion).

5.2 Tibiofemoral and patellofemoral contact forces

For maximum isometric extension of the model knee, peak forces exerted at the patellofemoral joint are higher than those which act between the femur and tibia (Fig. 5, compare PF and TF). At 90 ° of flexion, patellofemoral contact forces approach 11,000 N or 13 times body weight (Fig. 5, PF). Peak tibiofemoral forces occur at around 70° of flexion and are somewhat lower (Fig. 5, TF). The resultant force acting between the femur and tibia exceeds 6000 N or 8 times body weight. Notice, however, that the resultant patellofemoral contact force is lower than the resultant tibiofemoral contact force near full extension of the knee (compare PF and TF in the region 0-30 °). The reason is that, near full knee extension, the orientation of the patella is such that the applied quadriceps force is more-or-less equal to the force transmitted to the patellar ligament (not shown). Consequently, the forces acting normal to the patellar facet remain relatively small at small angles of the knee. Therefore, nearly all of the force in the patellar ligament acts to press the tibia and femur together, as the major component

of this force is directed along the long axis of the tibia at small angles of knee flexion.

Patellofemoral contact forces increase with knee flexion because quadriceps force increases. Quadriceps force increases because of the force -length properties of these muscles (Fig. 4, Quad). In fact, the shape and magnitude of the patellofemoral contact force is very similar to that of the applied quadriceps force. Shelburne and Pandy (1997) have shown that patellofemoral contact forces near full knee extension are governed by the geometry of the patellofemoral joint, and, more specifically, by the shapes of the patellar facet and femoral groove. At large angles of the knee, however, patellofemoral contact forces are determined almost exclusively by the force -length properties of the quadriceps muscles.

It is interesting to note that the forces acting at the medial and lateral sides of the knee not only have the same shape, but also have nearly equal magnitudes over the entire range of knee flexion (Fig. 5, compare dashed and dotted lines). Peak forces at each side of the tibiofemoral joint occur near 70° of flexion, and approach 3000 N or 4 times body weight. Tibiofemoral forces are small at small angles of the knee because the force applied by the quadriceps muscles is lowest here. The forces at the medial and lateral sides of the knee initially increase with increasing knee flexion because quadriceps force increases (compare TF in Fig. 5 with Quads in Fig. 4). In the region 60-90° of flexion, however, tibiofemoral forces decrease. This results from a sharp decrease in the force transmitted to the patellar ligament at large angles of knee flexion (not shown). The variation in patellar ligament force at large angles of flexion is determined by the geometry of the tibiofemoral joint, and, more specifically, by the shapes of the femoral condyles and tibial plateaux.

5.3 Ligament forces

The model ACL is loaded from 65° of flexion to full extension during maximum isometric knee extension (Fig. 6, aAC and pAC). There is some discrepancy between this result and those obtained from measurements of ligament strain,

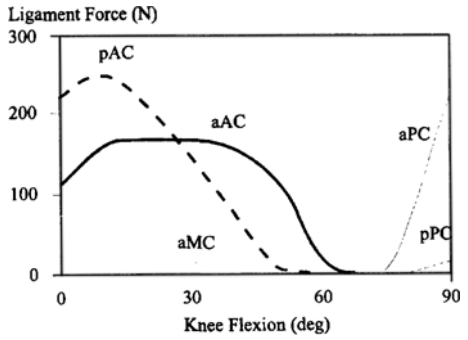

Fig. 6 Cruciate ligament forces calculated for maximum isometric extension of the model knee (aAC, heavy solid line; pAC, heavy dashed line; aPC, light solid line; pPC, light dashed line); aMC, dotted line.

which show that the ACL is loaded from 45° to full extension (Renstrom et al., 1986; Durselen et al., 1995). This difference is most likely explained by the fact that quadriceps forces applied in the experiments are much lower than those present during maximum voluntary contractions of the quadriceps.

The force in the model aAC increases from 65° of flexion, peaks in the range 20-40°, and then decreases as the knee approaches full extension (Fig. 6, aAC). A similar pattern of force is shown for the pAC, but this bundle develops higher forces near full extension, and is recruited at a smaller angle of knee flexion (Fig. 6, pAC). In general, load sharing between the separate bundles of the cruciate ligaments is determined by the angle at which each bundle meets the tibial plateau, and by the values of their resting lengths and stiffnesses. The interaction between each of these parameters in the model determines the distribution of force within the ligament. The changing distribution of bundle forces with knee flexion shown in Fig. 6 supports the contention that single-stranded reconstructions may not adequately meet the functional requirements of the natural ACL (Zavatsky and O'Connor, 1992). We note here that the total force in the model ACL remains below the limit estimated for ligament failure. Peak ACL force in the model reaches 400 N at 15° of flexion, which is lower than the maximum strength of human knee liga-

ment in either young or old specimens (1730 N and 734 N, respectively) (Noyes and Grood, 1976).

In agreement with the experimental findings of Hirokawa et al. (1992) and Wascher et al. (1993), the model PCL is loaded only beyond 70° of flexion during maximum isometric extension (Fig. 6, aPC). Notice that the forces in the PCL are higher for isometric extension than for a quadriceps leg raise. This prediction of the model is supported by the experiments of Wascher et al. (1993), who showed that quadriceps forces applied at large angles of knee flexion always increase total PCL force. The reason is that at large flexion angles in the model, as in the natural knee, the shear forces exerted by the patellar ligament, by the tibiofemoral contact, and by the restraining force, all induce a posterior shear force on the tibia (Daniel et al., 1998). This also explains why the force in the model ACL is zero at flexion angles greater than 65°.

The forces in the model collateral ligaments and capsule are all much smaller than those borne by the cruciate ligaments at all angles of the knee. MCL, LCL, and capsular forces added together are typically less than 5% of the resultant force in the model ACL, which is consistent with the view that the ACL provides the primary restraint to anterior drawer (Butler et al., 1980).

6. Maximum Isometric Knee Flexion

6.1 Flexor torque

Torques for maximum isometric flexion of the model knee also fell within the range of the values measured for the subjects (Fig. 7, compare heavy solid line with shaded region). Peak torques for the model and the subjects are lower than the corresponding values for maximum isometric extension, and they occur between 20° and 30° of flexion. Good agreement between model and experiment in these respects suggests that the parameters chosen for the hamstrings and gastrocnemius muscles in the model are reasonable. However, minor differences are also apparent. For example, maximum flexor torque for the model increases near full extension, whereas the

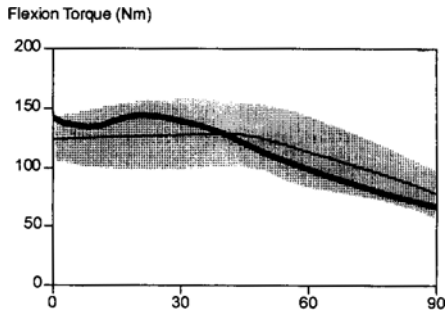

Fig. 7 Maximum, isometric, knee-flexor, torque-angle curves for the model (heavy solid line) and for human subjects (shaded region). The thin solid line represents the mean of all the experimental measurements. The shaded region represents ±1 standard deviation of the total flexor torques measured for the subjects during maximum, voluntary, isometric contractions of the hamstrings and gastrocnemius muscles.

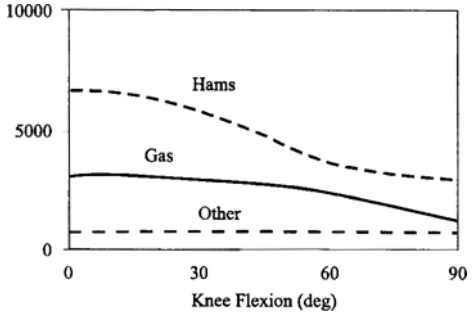

Fig. 8 Forces developed by all the knee flexor muscles included in the model during maximum isometric flexion. Hams (heavy solid line) represents the resultant force developed by all the hamstrings muscles in the model; Gas, (dashed line) represents the resultant force in gastrocnemius; Other (dotted line) is the resultant force in the remaining flexor muscles in the model (i. e., sartorius and gracilis).

experimental data remain relatively constant. Furthermore, maximum flexor torque generated by the model is somewhat lower than the average maximum values generated by the subjects at large angles of flexion.

Maximum isometric flexor torques are maximum near full extension and decrease monotonically as knee flexion increases. Knee

flexor torques are largest near full extension because the forces developed by the hamstrings and gastrocnemius muscles are maximum in this region (Fig. 8, Hams and Gas). Except for BFSH and BFLH, the moment arms of these muscles remain relatively constant throughout the range of knee flexion. Furthermore, the resultant force developed by the hamstrings is larger than that developed by gastrocnemius, implying that the hamstrings muscles dominate knee flexor torque at all angles of flexion.

6.2 Tibiofemoral contact forces

No experimental data are available in the literature for the forces acting between the femur and tibia during maximum contractions of the flexor muscles. The model calculations show that the resultant force acting between the femur and tibia during maximum isometric knee flexion is maximum at full extension of the knee. Peak tibiofemoral force for the model is around 5000 N or 6.5 times body weight (Fig. 9, solid line at full knee extension), which is slightly lower than the value calculated for maximum isometric knee extension. For maximum contractions of the quadriceps muscles, the resultant peak tibiofemoral contact force for the model was around 8 times body weight at 70° of knee flexion. As with maximum isometric knee extension, the forces exerted at the medial and lateral compartments of the knee are similar in both shape and magnitude. Both are maximum near full extension of the knee, and decrease to about half their maximum value at 90° of flexion.

Muscles dominate the resultant force acting between the bones during isometric contractions of the flexor muscles. For example, the peak force acting at the tibiofemoral joint at full extension is about 5000 N (Fig. 9, TF). At this position of the knee, the combined contribution from the forces acting in the hamstrings and gastrocnemius is around 4500 N. These results suggest that the forces transmitted to the ligaments and capsular structures of the knee contribute relatively little to the resultant force acting at the joint.

The resultant force acting between the femur and tibia during maximum isometric flexion is

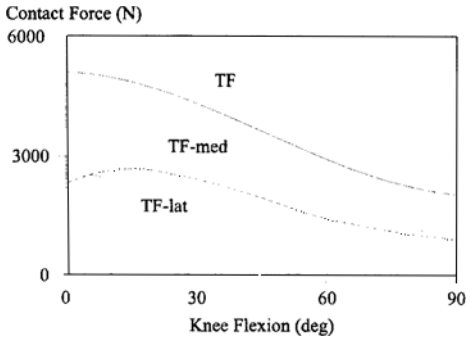

Fig. 9 Articular contact forces for maximum isometric flexion of the model knee. Resultant force acting at the tibiofemoral joint in the model (TF, solid line). The forces acting at the medial and lateral sides of the tibiofemoral joint are also shown.

dominated by the force developed in the hamstrings muscles. Hamstrings muscle force is maximum at full extension of the knee, after which it decreases monotonically as the knee flexes. This explains the observed variation in the tibiofemoral contact force with knee flexion. Because the force in gastrocnemius is much lower than hamstrings force at small knee angles, only hamstrings muscle force contributes substantially to the resultant force at the tibiofemoral joint. At knee flexion angles beyond 60°, however, both gastrocnemius and hamstrings forces contribute to the resultant force acting between the femur and tibia, as the difference in the magnitudes of these forces then becomes much smaller.

6.3 Ligament forces

Except near full extension, the forces in the separate bundles of the model ACL are zero for maximum isometric knee flexion (Fig. 10, aAC and pAC). Furthermore, ACL forces for isometric flexion are much lower than those calculated for extension. These results compare favorably with measurements of ACL strain reported by Beynnon et al. (1995). These researchers found that isolated hamstrings forces produced lower values of ACL strain at nearly all knee angles compared with values measured for passive extension. They found also that hamstrings forces alone cannot unload the ACL from

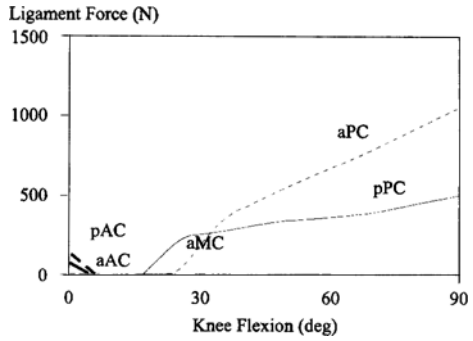

Fig. 10 Cruciate ligament forces calculated for maximum isometric flexion of the model knee (aAC, heavy solid line; pAC, heavy dashed line; aPC, light solid line; pPC, light dashed line); aMC, dotted line.

15° to full extension, which agrees well with our calculated range of 0-10° of knee flexion (Fig. 10, aAC and pAC from 0-10°).

In agreement with the calculations and experimental results of others (Hirokawa et al., 1992), the model PCL is loaded for almost the entire range of flexion; both bundles remain slack only from 20° of knee flexion to full extension (Fig. 10, aPC and pPC). Although total PCL forces for maximum isometric flexion are generally much higher than those calculated for extension, peak force in the model PCL remains below the level expected for ligament failure.

7. Conclusion

A major objective of the present work was to develop a realistic, three-dimensional mathematical model of the human knee joint and to integrate such a model into a detailed human musculoskeletal lower extremity model. This model provided a quantitative assessment of muscle and ligament function during human movement. Specifically, the model was used to determine the muscle, ligament, and articular contact forces transmitted at the knee as humans extend/flex in a isometric state.

The most significant contribution of the model is that it takes into account the effects of muscletendon properties and musculoskeletal geometry on calculations of ligament and joint-contact forces at the knee. Previous attempts to model the knee either have represented muscles as ideal force generators or have neglected their involvement altogether. Most attempts to include the effects of musculoskeletal geometry also have idealized the paths of the muscles as straight lines joining the insertion sites of the tendons. Our model not only incorrporates the force-length properties of all the major extensor and flexor muscles of the knee, but it also represents the path of each actuator more precisely.

Many of predictions made by the model follow the results of experiments reported by others. For a distal arrangement of the restraining pad, the model ACL is loaded from 70 deg of flexion to full extension during maximum isometric extension. Quadriceps-strengthening exercises such as maximum isometric knee extension should therefore be avoided in this region of flexion if the ACL is to be protected from the strain. In contrast, contractions of the hamstrings and gastrocnemius muscle protected the ACL for almost the entire range of knee flexion. Near full extension, the hamstrings could not supply a large enough posterior shear to overcome the anterior drawer created by the the restraining force and the tibiofemoral contact force, as the hamstrings all meet the tibia at relatively small angles near full extension of the knee. Hamstring-strengthening exercises can therefore be performed safely subsequent to ACL reconstruction, provided that these muscles are activated with the knee flexed to 10 deg or greater.

References

Beynnon, B. D., Fleming, B. C., Johnson, R. J., Nicoles, C. E., Renstrom, P. A., and Pope, M. H, 1995, "Anterior Cruciate Ligament Strain Behavior During Rehabilitation Exercises In vivo," *Am. J. Sports Med.*, Vol. 16, pp. 113~122.

Butler, D. L., Noyes, F. R., Grood, E. S., 1980, "Ligamentous Restraints to Anterior-Posterior Drawer in the Human Knee," *J. Bone Jt. Surg.*, Vol. 62-A, pp. 259~270.

Collins, J., and O'Connor, J., 1991, "Muscle-Ligament Interactions at the Knee During Walk-

ing," *Proc. Instn. Mech. Engrs.*, Part H, 205, pp. 11~18.

Daniel, D. M., Stone, M. L., and Riehl, B., 1988, "Use Of the Quadriceps Active Test to Diagonose Posterior Cruciate Ligament Disruption and Measure Posterior Laxity of the Knee," *J. Bone Jt. Surg.*, Vol. 70A, pp. 386~391.

Delp, S. L., 1990, "Surgery simulation: A Computer Graphics System to Analyze and Design Musculoskeletal Reconstructions of the Lower Limb," Ph. D. Thesis, Dept. of Mechanical Engineering, Stanford University.

Durselen, L., Claes, L., and kiefer, H., 1995, "The Influence of Muscle Forces and External Loads on Cruciate Ligament Strain," *Am. J. Sports Med.*, Vol. 23, pp. 129~136.

Freiderich, J. and Brand, R. A., 1990, "Muscle Fiber Architecture in the Human Lower Limb," *J. Biomechanics*, Vol. 23, pp. 91~95.

Hefzy, M. S. and Grood, E. S., 1988, "Review of Knee Model," *Appl. Mech. Rev.*, Vol. 41, pp. 1~13.

Hirokawa, S., Solomonow, M., Lu, Y., Lou, Z., and D'Ambrosia, 1992, "Anterior-Posterior and Rotational Displacement of the Tibia Elicited by Quadriceps Contraction," *Am. J. Sports Med.*, Vol. 20, pp. 299~306.

Kim, S., 1998, "Three-Dimensional Dynamic Model of the Human Knee," KSME International Journal Vol. 12, No. 6.

Kim, S., 1996, "A Three-Dimensional Dynamic Musculoskeletal Model of the Human Knee Joint," Ph. D. Dissertation, Mechanical Engineering Dept. The University of Texas at Austin, TX, U. S. A

Markolf, K. L., Gorek, J. F., Kabo, M. et al., 1990, "Direct Measurement of Resultant Forces in the Anterior Cruciate Ligament," *J. of Bone Jt. Surg.*, Vol. 72-A, pp. 557~567.

Pandy, M. G., Zajac, F. E., Sim, E., and Levine, W. S., 1990, "An Optimal Control Model for Maximum-Height Human Jumping," *J. Biomechanics*, Vol. 23, pp. 1185~1198.

Renstrom, P., Arms, S., Stanwyck, T., Johnson, R., and Pope, M., 1986, "Strain Within the Anterior Cruciate Ligament During Hamstrings and Quadriceps Activity," *Am J Sports Med.*, Vol. 14, pp. 83~87.

Shelburne, K. B. and Pandy, M. G., 1997, "A Musculoskeletal Model of the Knee for Evaluating Ligament Forces During Isometric Contractions," *J. Biomechanics*, Vol. 30, pp. 163~169.

Wascher, D. C., Markolf, K. L., Shapiro, M. S., and Finerman, G. A., 1993, "Direct In vitro Measurement of Forces in the Cruciate Ligaments. Part 1: The Effect of Multiplane Loading in the Intact Knee," *J. Bone Jt. Surg.*, Vol. 75-A, pp. 377~386.

Zavatsky, A. B. and O'Connor, J. J., 1993, "Ligament Forces at the Knee During Isometric Quadriceps Contractions," *Proc Instn Mech Engrs.*, Part H 207, pp. 7~18.